Shear-Induced Concentration Fluctuations in Ultrahigh Molecular Weight Polyethylene Solutions. 1. Observation above the Melting Point

Hiroki Murase, Takuji Kume, and Takeji Hashimoto*

Department of Polymer Chemistry, Graduate School of Engineering, Kyoto University, Kyoto 606−01, Japan

Yasuo Ohta and Tohru Mizukami

TOYOBO Research Institute, TOYOBO Co., Ltd., 2-1-1, Katata, Ohtu-shi, Shiga 520-02, Japan

Received June 12, 1995; Revised Manuscript Received August 7, 1995[⊗]

ABSTRACT: The shear-induced concentration fluctuations in semidilute solutions comprised of ultrahigh molecular weight polyethylene (UHMWPE) as a solute and paraffin as a solvent were studied by shear−small-angle light scattering and shear−microscopy. In steady-state shear flow, a unique anisotropic scattering pattern was found to appear when the shear rate $\dot{\gamma}$ is increased above a critical shear rate $\dot{\gamma}_c$. This anisotropic scattering pattern was found to be essentially identical to the "butterfly pattern" observed in high molecular weight polystyrene solutions in dioctyl phthalate. This butterfly pattern, found at temperatures higher than the equilibrium melting temperature of UHMWPE, suggests that the shear-induced concentration fluctuations or phase separation occurs in the homologous mixtures of UHMWPE and paraffin having characteristics of athermal solutions.

I. Introduction

When some semidilute polymer solutions in the one-phase region are subjected to flow, the solutions become turbid because of enhancement of concentration fluctuations or liquid−liquid phase separation induced by the flow. In recent years this flow-enhanced concentration fluctuations or flow-induced phase separation phenomenon has attracted a great deal of attention. Experimental[1−13] and theoretical studies[14−18] were carried out to gain insight into the physics underlying this intriguing nonequilibrium phenomenon.

Up to now most of the experimental studies have been confined to a particular system of semidilute polystyrene solutions with dioctyl phthalate as a solvent (PS/DOP). Here the thermodynamic interaction between polymer and solvent and the deformation of entangled polymers under flow play an important role in the observed phenomenon. At this stage it still may be important for us to extend the investigation of this intriguing phenomenon to a variety of polymer−solvent systems in order to check the universality of this phenomenon. To our knowledge, however, there are no studies which clearly prove the existence of the shear-induced liquid−liquid phase separation in semidilute crystallizable polymer solutions, although there are a large number of studies on the shear-induced crystallization,[19−25] i.e., liquid−solid phase transition. The report by McHugh et al.[24,25] may be an example of the exceptional cases which inferred the existence of the liquid−liquid phase separation of dilute solutions of polyethylene, polypropylene, and poly(ethylene oxide) immediately before the flow-induced crystallization takes place.

Thus in this work we attempt to investigate whether the shear-enhanced concentration fluctuations can be observed for semidilute solutions comprised of ultrahigh molecular weight polyethylene (UHMWPE) as a solute and paraffin as a solvent (UHMWPE/paraffin solutions) at temperatures higher than their melting points. This system is considered to be more interesting than the PS/DOP system from the viewpoint that UHMWPE and paraffin are chemically identical (homologous) to each other and hence form nearly athermal solutions. Recently published theory[18] suggests that flow-induced concentration fluctuations or phase separation will occur in polymer mixtures when the two components of the mixture have a large difference in their viscoelastic properties, even if the mixtures are comprised of chemically identical polymers. According to this theory, we should be able to observe the shear-induced phase separation also in UHMWPE/paraffin solutions.

The study is believed to be important also from the viewpoint of understanding the shear-induced crystallization of crystallizable polymer solutions. If the shear-induced concentration fluctuations occur prior to the crystallization, the crystallization should be further enhanced locally in the regions rich in polymers; thus the shear-enhanced concentration fluctuations may result in the shear-enhanced crystallization. This aspect on the crystallization has essentially long been overlooked in the history concerning the research of shear-induced crystallization.

In order to pursue this research, we have to overcome the following experimental difficulties: (i) the experiments have to be conducted at relatively high temperatures, higher than the melting temperatures of the solutions in the quiescent state, and (ii) parasitic scattering from the shear cell and from impurities in polyethylene solutions should be carefully avoided, because the polyethylene solutions have a scattering power much lower (about 2 orders of magnitude lower) than that of the PS/DOP solutions. The refractive index increment dn/dc is −0.001 mL/g for PE/paraffin at λ = 633 nm, 135 °C[26] and 0.119 mL/g for PS/DOP at λ = 514 nm, 25 °C.[27] Here we aim to present the first

* To whom correspondence should be addressed.

[⊗] Abstract published in *Advance ACS Abstracts,* October 1, 1995.

0024-9297/95/2228-7724$09.00/0

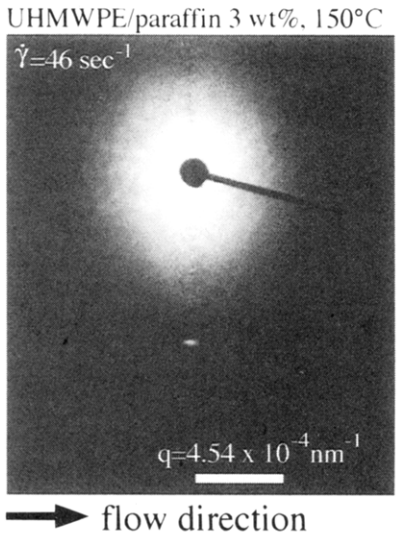

Figure 1. Example of the scattering pattern from the solution obtained without filtration of insoluble impurities. The solution is in steady-state shear flow of shear rate $\dot{\gamma} = 46$ s^{-1} at 150 °C. Intense parasitic scattering from the impurities overlays the true scattering pattern from the sheared solution. The flow direction is in the horizontal direction. The setup used in this experiment is shown in Figure 2.

experimental results in a series of our studies along this line.

II. Experimental Section

A. Sample. Commercial grade UHMWPE (Hizex 240M, Mitsui Petrochemical Industries Ltd.) was used for this experiment. The polymer has a weight-average molecular weight of $M_w = 2.0 \times 10^6$ and a heterogeneity index $M_w/M_n = 12$,[28] where M_n denotes the number-average molecular weight. Paraffin wax (Luvax 1266, Nippon Seiro Co. Ltd.) was used as solvent. The number-average molecular weight of the paraffin wax is approximately 500 (producer's specification; measured by gas chromatography) and its melting point is 69 °C.

B. Preparation of Solutions. The UHMWPE was dissolved in the paraffin wax with an antioxidant agent (2,6-di-*tert*-butyl-*p*-cresol), with amount 1 wt % of the total solution, using a screw-type extruder at 210 °C. Small particles (insoluble impurities) contaminating the solutions were filtered off by a mesh filter (400 lines/in.). This process was very important to obtain good scattering data. If we omit this process, intense scattering arising from the particles will disturb the light-scattering observation. Figure 1 shows the scattering pattern under steady-state shear flow from the solution obtained without the filtration. Diffuse parasitic scattering overlays the true scattering from the sheared solution. In the case of UHMWPE/paraffin solutions, scattered intensity is weak because of the small difference of refractive index between UHMWPE and paraffin (dn/dc is on the order of 10^{-3} mL/g[26] at 135 °C). Consequently, the parasitic scattering is a serious problem for scattering experiments. The solutions were subsequently extruded through a spinneret having a diameter of 0.8 mm at 160 °C. The extruded solutions were collected in glass vessels mounted 30 cm below the spinneret surface and gradually cooled to room temperature. The deformation memory imposed on the specimen in the extrusion process relaxed during the cooling process. Solutions containing 3 and 5 wt % of UHMWPE were prepared in this way.

C. Characteristics of the Solutions. The melting points of the obtained solutions were estimated by differential scanning calorimetry (DSC). Using a heating rate of 10 °C/min, the melting points were determined to be 115.9 and 116.9 °C for the 3 and 5 wt % solutions, respectively. The reduced concentrations C/C^* (C is the concentration of UHMWPE in solution and C^* is the overlap concentration) of these solutions

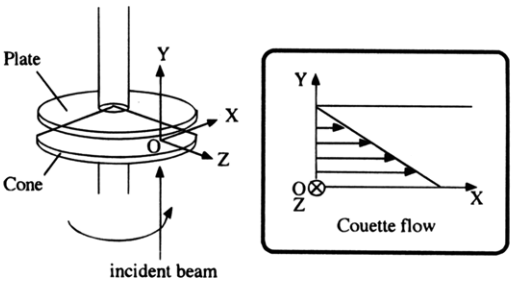

Figure 2. Transparent cone-and-plate shear cell and the coordinate system for the optical setup.

were approximately estimated by the following equations:[29]

$$\langle S^2 \rangle = (bL/3) - b^2 + (2b^3/L)\{1 - (b/L)[1 - \exp(-L/b)]\} \quad (1)$$

$$C^* = 3M/(4\pi \langle S^2 \rangle^{3/2} N_A) \quad (2)$$

$\langle S^2 \rangle$, b, L, M, and N_A are the mean-squared radius of gyration, the persistence length, the contour length, the molecular weight of UHMWPE, and the Avogadro number, respectively. Using 0.575 nm[30] for the persistence length b of polyethylene and 18 214 nm for the contour length L ($L = Md/28$, molecular weight $M = 2.0 \times 10^6$, and length of one ethylene unit $d = 0.255$ nm), $\langle S^2 \rangle$ is calculated as 3490 nm^2 and C^* as 3.85×10^{-3} g/cm^3 $\cong$ 0.45 wt %. Both the 3 wt % solution and the 5 wt % solution are in the semidilute state, and C/C^* are approximately 6.7 and 11.1, respectively.

D. Shear–SALS Method. The shear–SALS experiments were carried out using two types of shear–SALS apparatus.[31–33] The quantitative measurements of scattering intensity distribution with a photodiode array were carried out using the first type of apparatus.[31,32] The second type[33] was used to record the scattering patterns on photographic films. The optical setups of the two apparatuses were identical to those in previous reports.[31–33] A quartz-made cone-and-plate type shear cell (cone angle = 1°) was used in both apparatuses. A velocity gradient exists in the plane Oyx, where the Ox axis is in direction of the flow and the Oy axis is perpendicular to the plate surface of the shear cell and parallel to the velocity gradient direction (Figure 2). The Oz axis is parallel to the neutral axis or the vorticity direction. The incident beam was sent along the Oy axis.

The optically transparent shear cell was filled with the sample and subsequently heated to 150 °C. The temperature of the solutions was kept at 150 °C for over 1 h to allow relaxation of the deformation induced in the solutions during the process of filling of the sample in the shear cell. Steady shear flow with shear rate $\dot{\gamma}$ from $\dot{\gamma} = 0.046$ to 115 s^{-1} was imposed on the solution, and light-scattering data were collected after the scattering reached a steady-state scattering. It should be noted that the experimental temperature of 150 °C is higher than the melting points of these solutions and than the equilibrium melting temperature (146 °C) of bulk polyethylene. Therefore no crystallization occurred under this experimental condition.

The intensity distribution was qualitatively measured by using a photographic film (Fuji Neopan SS; ISO = 100) placed normal to the Oy axis. The scattering patterns recorded on the negatives were digitized with the image scanner (Epson GT-8000) with the transparency unit and their contour plots were calculated with a personal computer with a commercial software (Spyglass). The quantitative measurements of scattering intensity distribution were carried out by placing a linear photodiode array in the detector plane normal to the Oy axis and parallel to the Ox axis (flow direction). Here we report the scattering observed with a linearly polarized incident beam with the polarization direction normal to the flow direction, and no analyzer was placed between the shear cell and the detector.

E. Shear–Microscopy Method. As shown in the previous reports,[12,33] *in-situ* optical microscopic observations give useful information for the understanding of the structure

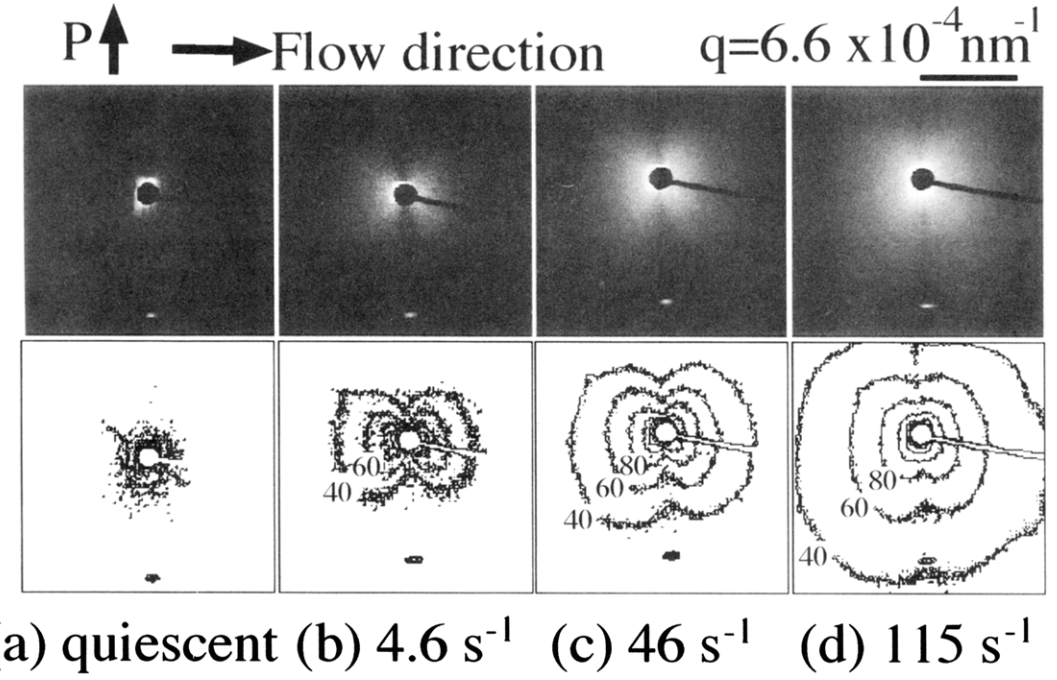

Figure 3. Scattering patterns recorded on photographic films and their contour plots from the 3 wt % UHMWPE/paraffin solution under steady-state shear flow at various shear rates. The patterns were taken *in situ* with an exposure time of 1/60 s. The incident laser beam is linearly polarized, and its polarization axis is normal to the shear flow direction as indicated by the arrow (analyzer was not used). The numbers inserted in the contour lines indicate the relative scattering intensity levels (arbitrary unit).

formation under shear flow. Thus we applied the shear–microscopy method on the UHMWPE solutions. A white halogen lamp was used as a light source. The optical axis of the microscope was aligned parallel to the Oy axis and therefore the structure development in the Oxz plane was observed. It should be noted that the direction of the incident beam for the microscopic experiments is equivalent to that of the shear–SALS experiments. Therefore the observed structures are the same and allow a comparison of the two results. A fast shutter (as fast as 1/10000 s) CCD video camera (Sony SSC-M370) was connected to the optical microscope. The images were recorded on videotape by an SVHS VCR (Victor HR-S6600) as an analog movie and digitized with a frame grabber board (RasterOps 24STV) mounted on a Macintosh computer. In this case, any object observed in the sight of the optical microscope moves not more than 0.3 μm parallel to the flow direction during 1/10000 s. This distance was acceptably small compared with the size of the structures developed in the solution. The micrographs were saved digitally by an image processing system. Thus the fast Fourier transform (FFT) can be carried out from the images. The FFT images were used to confirm whether the microscope images are a true representation of structural entity under flow by comparing the FFT spectrum with the corresponding light-scattering patterns.

III. Results and Discussion

Figures 3 and 4 show, respectively, a series of scattering patterns under steady shear flow at a temperature of 150 °C for 3 and 5 wt % solutions of UHMWPE/paraffin as a function of shear rate $\dot{\gamma}$. The top pictures are original scattering patterns recorded on photographic films with an exposure time of 1/60 s and the bottom plots are their contour plots. The numbers inserted in the contour plots indicate scattering intensity at each contour line (arbitrary unit), showing the relative intensity distribution in the scattering patterns. As shown in Figures 3a and 4a, the scattering intensity in the quiescent state is very weak and isotropic, because the solution is in the one-phase state where the polymer dissolves in the solvent homogeneously. When the solution was subjected to shear flow, a unique anisotropic scattering pattern appeared (Figures 3b–d and 4b–d). This anisotropic scattering pattern has a remarkable feature: no or very weak scattering appears along the azimuthal angle $\mu = 90°$ (normal to the shear flow) and strong scattering occurs along $\mu = 0°$ (parallel to the flow), giving rise to a sharp "dark streak" along $\mu = 90°$. This pattern is similar to the scattering pattern designated as the "butterfly pattern" observed in polystyrene/dioctyl phthalate (PS/DOP) solutions.[7,8,12] With increasing $\dot{\gamma}$, the scattering intensity of the butterfly pattern increases and the butterfly wings spread forward $\mu = 90°$, giving rise to an increasingly sharp dark streak. Comparing the scattering patterns of the 3 and 5 wt % solutions, the shape of the pattern and its change with $\dot{\gamma}$ are fundamentally similar. The 5 wt % solution, however, seems to have a higher intensity than the 3 wt % solution at the same $\dot{\gamma}$, which is more clearly represented in Figure 5.

Figure 5 shows the double-logarithmic plot of the integrated scattered intensity parallel to the flow direction $\mathcal{I}_{\parallel}(\dot{\gamma})$ as a function of the shear rate $\dot{\gamma}$. The integration was carried out from $q = 6.3 \times 10^{-4}$ to 1.78 $\times 10^{-3}$ nm^{-1}. $\mathcal{I}_{\parallel}(\dot{\gamma})$ was normalized with respect to the intensity in the quiescent state, $\mathcal{I}_{\parallel}(\dot{\gamma}=0)$. On both the 3 wt % solution and the 5 wt % solution, the scattered intensity $\mathcal{I}_{\parallel}(\dot{\gamma})$ dramatically increased with shear rate $\dot{\gamma}$ when $\dot{\gamma}$ was increased above the critical shear rate $\dot{\gamma}_c$, indicated by vertical arrows in Figure 5. The critical shear rate $\dot{\gamma}_c$ was assessed as $\dot{\gamma}$ above which $\mathcal{I}_{\parallel}$ starts deviating from unity. More precisely, $\dot{\gamma}_c$ was determined as the value at which the straight line fitted to the data points which clearly indicate $\mathcal{I}_{\parallel}(\dot{\gamma})/\mathcal{I}_{\parallel}(\dot{\gamma}=0)$ deviating from unity intersects the baseline, representing $\log[\mathcal{I}_{\parallel}(\dot{\gamma})/\mathcal{I}_{\parallel}(\dot{\gamma}=0)] = 0$. The scattering intensity of the 5 wt % solution is several times higher than that of the 3 wt % solution at $\dot{\gamma} > \dot{\gamma}_c$. The $\dot{\gamma}_c$ shifts from 0.2 to 0.05 s^{-1} with increase of the polymer concentration from 3 to 5 wt %. This concentration dependence of $\dot{\gamma}_c$ is qualitatively equivalent to those observed in PS/DOP solutions.[7]

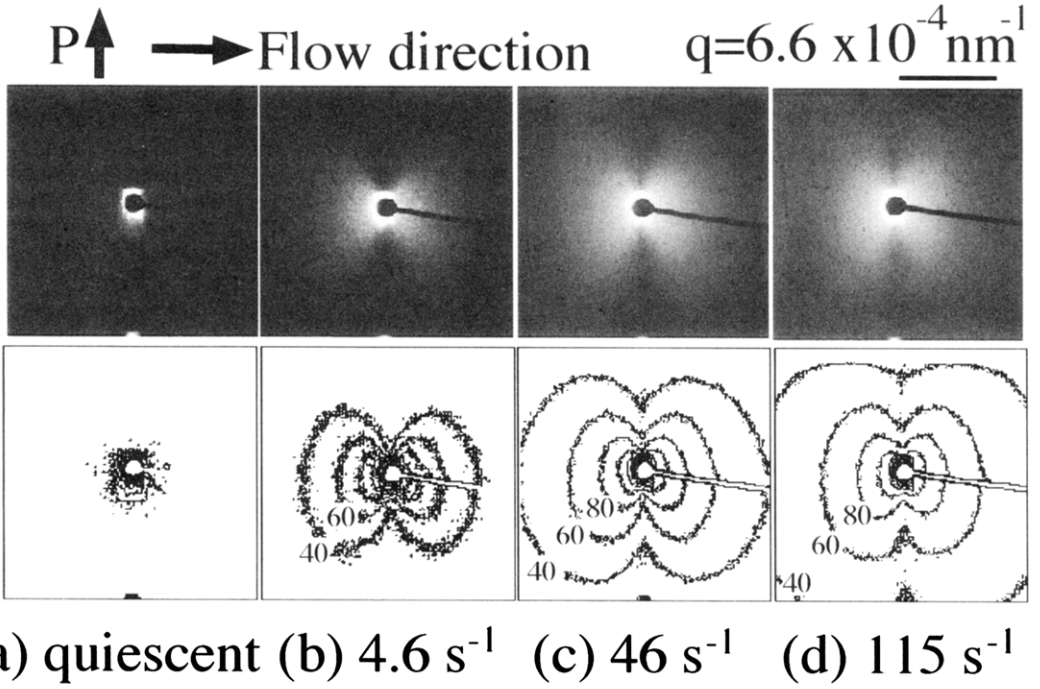

Figure 4. Scattering patterns recorded on photographic films and their contour plots from the 5 wt % UHMWPE/paraffin solution under steady-state shear flow at various shear rates. The patterns were taken *in situ* with an exposure time of 1/60 s. The incident laser beam is linearly polarized, and its polarization axis is normal to the shear flow direction as indicated by the arrow (analyzer was not used). The numbers inserted in the contour lines indicate the relative scattering intensity levels (arbitrary unit).

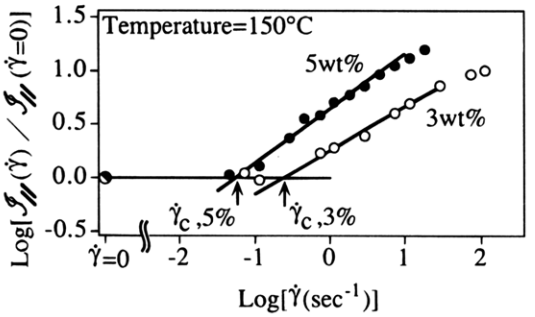

Figure 5. Normalized integrated scattered intensity parallel to the flow as a function of shear rate $\dot{\gamma}$ for 3 and 5 wt % solutions at 150 °C. The arrows show the critical shear rate $\dot{\gamma}_c$ for the onset of the shear-induced concentration fluctuations. The $\dot{\gamma}_c$ was obtained as the value at which the straight line fitted to the data points, which clearly indicate $\mathcal{I}(\dot{\gamma})/\mathcal{I}(\dot{\gamma}=0)$ deviating from unity, intersects the baseline, representing $\log[\mathcal{I}(\dot{\gamma})/\mathcal{I}(\dot{\gamma}=0)] = 0$.

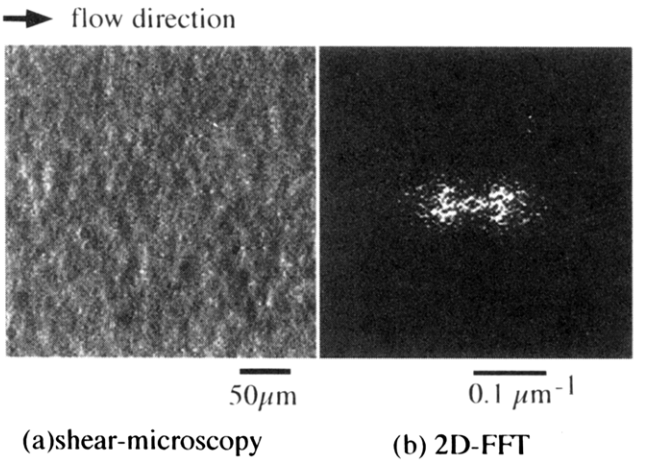

Figure 6. Optical micrograph taken under steady-state shear flow at 150 °C: (a) bright-field optical micrograph of UHMWPE/paraffin having 5 wt % polymer concentration at a shear rate of 4.6 s^{-1}; (b) computed fast Fourier transform (FFT) spectrum from the micrograph.

Figure 6 shows an optical micrograph taken for the 5 wt % solution under steady shear flow. The experimental condition used is same as that used for the light-scattering experiment. The left-hand micrograph (Figure 6a) is a bright-field optical micrograph obtained under steady shear flow at $\dot{\gamma} = 4.6\ s^{-1}$, and the right-hand pattern (Figure 6b) is its computed FFT power spectrum (calculated by NIH Image[34]). In the optical micrograph, periodic ripples having the characteristic length scale of about 25 μm appear parallel to the flow axis Ox. The FFT spectrum shows a similar feature with the butterfly pattern observed in the light-scattering experiment shown in Figure 4b. Therefore, these ripples must be the structure which causes the butterfly pattern in the light-scattering experiment. They are expected to reflect the shear-enhanced concentration fluctuations.

To elucidate the structural detail of the ripples, we applied image processing on the micrograph. Figure 7a is a close-up of Figure 6. At first the original image was transformed into Fourier space with FFT, whose spectrum here is denoted as $I_{FFT}(\mathbf{q})$. Next we applied a frequency filter on the FFT spectrum. The filter function is denoted by $F(\mathbf{q})$. In order to obtain this filter function, $I_{FFT}(\mathbf{q})$ was first smoothed and a contour line with an isointensity level of $0.85I_{max}$ was constructed from the smoothed spectrum defined by $I^s_{FFT}(\mathbf{q})$, where I_{max} is the maximum intensity of $I^s_{FFT}(\mathbf{q})$. We created a region based on the contour line. $F(\mathbf{q})$ was set to 1 if $\mathbf{q}$ locates inside this region and 0.3 if $\mathbf{q}$ locates outside. The filtered FFT spectrum $I^f_{FFT}(\mathbf{q})$ was obtained as a product of $F(\mathbf{q})$ and $I_{FFT}(\mathbf{q})$. Figure 7b shows this filtered FFT spectrum. Finally, a filtered real-space image was reconstructed from the filtered spectrum $I^f_{FFT}(\mathbf{q})$ through inverse FFT. In such image filtration we can extract and enhance the structure giving rise to the butterfly-shape spectrum from the original image.

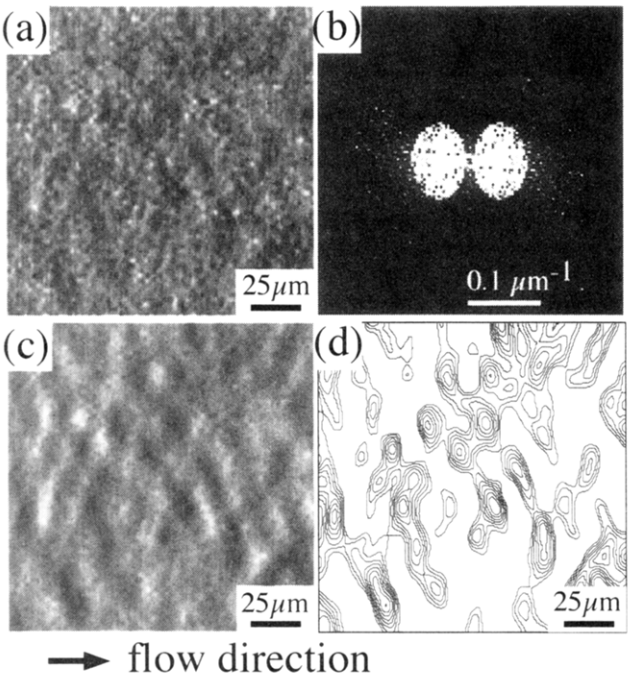

Figure 7. Image extraction from the optical micrograph: (a) original micrograph; (b) filtered FFT spectrum extracted from the original FFT spectrum obtained from the micrograph in (a); (c) reconstructed image through inverse FFT of the filtered FFT spectrum; (d) contour map showing brightness distribution in the image (c). The contour map represents the area having a brightness lower than average.

Panels c and d of Figure 7 are the filtered optical image and its contour map for the brightness distribution, respectively. The contour image represents the area having a brightness lower than average.

Parts c and d of Figure 7 show the specific feature of the ripples having continuity normal to shear flow. The feature of ripples is basically similar to those observed in the PS/DOP system.[12] Such a feature of ripples is interpreted to represent the spatial concentration fluctuations that is enhanced in the shear flow direction. The continuity of the contour image normal to the shear flow direction suggests that the concentration fluctuations remain unaltered from the quiescent state in the direction perpendicular to the flow because of the absence (or weakness) of a driving force for the shear enhancement of the concentration fluctuations in this direction.

Shear-induced concentration fluctuations have so far been examined mainly for PS/DOP. This phenomenon has been interpreted to arise from the elastic effect[14-18] in entangled polymer solutions, i.e., a coupling between stress and concentration fluctuations through the concentration-dependent normal stress coefficient and viscosity. In PS/DOP systems the concentration fluctuations depend on the Flory–Huggins interaction parameter χ between PS and DOP. Thus the thermodynamic interaction and the shear flow affect the shear-induced concentration fluctuations for a given solution at a given temperature. As shown above, we can see the appearance of a butterfly-type scattering pattern under shear flow on UHMWPE/paraffin solutions. The results indicate the striking similarity between UHMWPE/paraffin and PS/DOP in terms of both scattering and microscope image. In contrast to PS/DOP, in the UHMWPE/paraffin system, the solvent (paraffin) has the same chemical structure as UHMWPE, and the solvent and the polymer are different only in the degree of polymerization. Thus they must form an essentially athermal solution; i.e., the interaction parameter between the polymer and the solvent is essentially zero. Thus this system provides an ideal system for studying the elastic effects on the shear-induced concentration fluctuations: in this system, the difference in rheological response between UHMWPE and paraffin can be a main physical factor affecting the shear-induced concentration fluctuations.

Since the experiments were carried out above the equilibrium melting temperature of UHMWPE, the scattering should be free from shear-induced crystallization. In fact, the scattered intensity was found to be independent of the polarization direction of the incident beam, and no appreciable scattering was observed under crossed polarizers.

IV. Conclusions

Shear-induced concentration fluctuations in semidilute solutions comprised of ultrahigh molecular weight polyethylene as a solute and paraffin as a solvent (UHMWPE/paraffin solutions) were studied by using the techniques of shear–small-angle light scattering (shear–SALS) and shear–microscopy. We succeeded in finding that UHMWPE/paraffin solutions in the single-phase state in the absence of shear show a unique anisotropic scattering pattern under shear flow at temperatures higher than the equilibrium melting temperature T_{me} of UHMWPE and identifying that the pattern is identical to the "butterfly pattern" observed in polystyrene/DOP solutions. A simultaneous observation with the shear–microscopy and the image analysis of the micrographs clearly indicated that the butterfly-type scattering pattern reflects the occurrence of shear-enhanced concentration fluctuations parallel to the flow direction as shown in Figure 7d. The characteristic wavelength of the fluctuations is on the order of 20 μm. UHMWPE and paraffin have the same chemical structure and differ only in the degree of polymerization. Thus the difference in rheological response of UHMWPE and paraffin due to the difference in their chain length plays an important role for the shear-induced concentration fluctuations.[18] Studies of this phenomenon are anticipated to be very important in terms of the shear-induced crystallization as well when the solutions are sheared at temperatures lower than T_{me} of the solutions. Studies along this line are also in progress in our laboratory.

References and Notes

(1) Larson, R. G. *Rheol. Acta* **1992**, *31*, 497.
(2) Ver Strate, G.; Phillipoff, W. *J. Polym. Sci. Polym. Lett.* **1974**, *12* , 267.
(3) Schmidt, R.; Wolf, B. A. *Colloid. Polym. Sci. Polym. Lett. Ed.* **1979**, *257*, 1188.
(4) Rangel-Nafaile, C.; Metzner, A. B.; Wissbrun, K. F. *Macromolecules* **1984**, *17*, 1187.
(5) Krämer-Lucas, H.; Schenck, H.; Wolf, B. A. *Makromol. Chem.* **1988**, *189*, 1613.
(6) Wu, X. L.; Pine, D. J.; Dixon, P. K. *Phys. Rev. Lett.* **1991**, *66*, 2408.
(7) Hashimoto, T.; Fujioka, K. *J. Phys. Soc. Jpn.* **1991**, *60*, 356.
(8) Hashimoto, T.; Kume, T. *J. Phys. Soc. Jpn.* **1992**, *61*, 1839.
(9) van Egmond, J. W.; Werner, D. E.; Fuller, G. G. *J. Chem. Phys.* **1992**, *96*, 7742.
(10) van Egmond, J. W.; Werner, D. E.; Fuller, G. G. *Macromolecules* **1993**, *26*, 7182.
(11) Moldenaers, P.; Yanase, H.; Mewis, J.; Fuller, G. G.; Lee, C.-S.; Magda, J. J. *Rheol. Acta* **1993**, *32*, 1.
(12) Moses, E.; Kume, T.; Hashimoto, T. *Phys. Rev. Lett.* **1994**, *72*, 2037.
(13) Boue, F.; Lindner, P. *Europhys. Lett.* **1994**, *25*, 421.

(14) Helfand, E.; Fredrickson, G. H. *Phys. Rev. Lett.* **1989**, *62*, 2468.
(15) Onuki, A. *Phys. Rev. Lett.* **1989**, *62*, 2472; *J. Phys. Soc. Jpn.* **1990**, *59*, 3427.
(16) Milner, S. T. *Phys. Rev. Lett.* **1991**, *66*, 1477.
(17) Mavrantzas, V. G.; Beris, A. N. *Phys. Rev. Lett.* **1992**, *69*, 273.
(18) Doi, M.; Onuki, A. *J. Phys. II Fr.* **1992**, *2*, 1631.
(19) Pennings, A. J.; Kiel, A. M. *Kolloid Z. Z. Polym.* **1965**, *205*, 160.
(20) Keller, A.; Machin, M. J. *J. Macromol. Sci., Phys.* **1967**, *B1*, 41.
(21) Pennings, A. J.; van der Mark, J. M.; Booij, H. C. *Kolloid Z. Z. Polym.* **1970**, *236*, 99.
(22) Frank, F. C.; Keller, A.; Mackley, M. R. *Polymer* **1971**, *12*, 467.
(23) Pennings, A. J. *J. Polym. Sci., Polym. Symp.* **1977**, *59*, 55.
(24) McHugh, A. J.; Blunk, R. H. *Macromolecules* **1986**, *19*, 1249.
(25) McHugh, A. J.; Spevacek, J. A. *J. Polym. Sci., Part B: Polym. Phys.* **1991**, *29*, 969.
(26) Horska, J.; Stejskal, J.; Kratochvil, P. *J. Appl. Polym. Sci.* **1979**, *24*, 1845.
(27) Link, A.; Springer, J. *Macromolecules* **1993**, *26*, 464.
(28) Hill, M. J. *Polymer* **1994**, *35*, 1991.
(29) Fujita, H. *Polymer Solutions*; Studies in Polymer Science 9; Elsevier: Amsterdam, 1990; Chapters 5 and 6.
(30) Erman, B.; Flory, P. J.; Hummel, J. P. *Macromolecules* **1980**, *13*, 484.
(31) Hashimoto, T.; Takebe, T.; Suehiro, S. *Polym. J.* **1986**, *18*, 123.
(32) Takebe, T.; Sawaoka, R.; Hashimoto, T. *J. Chem. Phys.* **1989**, *91*, 4369.
(33) Kume, T.; Asakawa, K.; Moses, E.; Matsuzaka, K.; Hashimoto, T. *Acta Polym.* **1995**, *46*, 79.
(34) NIH Image is the public domain Image program for a Macintosh computer written by Wayne Rasband at the U. S. National Institutes of Health. It is available from the Internet by anonymous ftp from zippy.nimh.nih.gov or on floppy disk from NTIS, 5285 Port Royal Rd., Springfield, VA 22161, part no. PB93-504868.

MA950824E